International Journal of Applied Engineering Research ISSN 0973-4562 Volume 10, Number 23 (2015) pp 43336-43344

Control of Compensation Devices by p-q, d-q and Fourier Control Methods to Improve the Power Quality in a Microgrid

A. Asuhaimi Mohd Zin[1a],A. Naderipour[2a],A. Khajehzadeh[3b] and M. H. Bin Habi Buddin[4a]

Professor[1], Ph.D Candidate[2], AssistantProfessor[3],Associate Professor[4]
[a]Faculty of Electrical Engineering, Universiti Teknologi Malaysia, 81310 Johor, MALAYSIA
eng.a.naderipour@ieee.org[1], asuhaimi@utm.my[2],.mdhafiz@utm.my[3]
[b]Department of Engineering Kerman Branch, Islamic Azad University, Kerman Iran
alikhajezadeh@yahoo.com

Abstract
The present study used passive filters (PF) and designed shunt active power filters (SAPFs) with three rife control methods: instantaneous reactive power theory (pq), the Synchronous Reference Frame (dq) and Fourier methods. Studies in the domain of microgrids include distributed generation sources and non-linear loads. Distributed generation sources include micro turbines (MT) and fuel cells (FC), which act as a source of harmonic currents with non-linear loads. To achieve this goal, passive filters are applied to cancel the main harmonics and to provide reactive power, whereas SAPFs are applied to adjust system imbalances and remove the remaining harmonics in the system. The results show that the method can reduce the harmonic disturbances of the system from 25.39% to less than 5%. In addition, this study analyzes how the various control methods operate on active filters. The proposed method has been validated experimentally, and the results are in agreement with the simulation results.

Keywords: Power quality, Microgrid, Harmonic, Dispersed generation, Active filter, Passive filter.

Introduction

Since the late 1980s, the importance of power quality has increased for electric supply companies and low and middle voltage consuming customers [1]. Due to the importance of some sources in the industry, they produce harmonics and act like non-linear loads. As non-linear consumers have increased, the effects of harmonics injected into the network have become more important [2]. The IEEE 519 standard specifies the limit of harmonic production for each consumer [3]. An effective method for harmonic suppression is harmonic compensation using passive [4]–[6], active power [7]–[10] and hybrid compensator filters [11]–[13]. On the other hand, distributed generation sources can be modeled as non-linear loads [14]. Installing passive filters in the appropriate locations, preferably close to the harmonic generator, can lead to trapping of the harmonic currents near the source and can reduce their distribution through the other parts of the system. Active filters, which are usually connected to a point of common coupling (PCC), can reduce the harmonics produced in the sources [15]. Combining these two filters leads to compensation for the insufficiencies of either. Some different controlling methods are used as active filters [16]. A microgrid can be connected to the utility grid at the PCC and is able to flexibly import/export energy from/to the grid [17]. Nadeem Jelani [18] proposed the possibility of using controlled industrial loads in a microgrid as active power filters. Different control strategies for active power filters under unbalanced conditions include IRP p-q and CPC-based time and frequency domain are given. Diarmaid J. Hogan [19] presented an adaptive current-control scheme for a three-phase APF for use within a microgrid. A vector-proportional-integral (VPI) controller with grid frequency tracking capabilities is used to compensate up to the 18th harmonic in the synchronous-reference-frame. This control scheme utilizes an advanced synchronous-reference frame phase-locked loop (SRF-PLL) to update the resonant frequency values of the current controllers to ensure the resonant frequency of the VPI remain at the optimum point regardless of changes in the grid frequency. D. Menniti [20] proposed the application of the strategy control approach used for the shunt active power filter previously proposed by the authors for the inverter interface of each single micro-source present in a microgrid.

The rest of this paper is divided as follows: this study applies the three control methods on the active filter using MATLAB software and the results are compared. The MT and FC are used as the distributed generation sources in the system in such a way that the sources are connected to the grid by AC/DC/AC and AC/DC convertors, and a harmonic current is injected into the grid.

Structure of the System

Fig. 1 displays the configuration of the studied system. The active filter is integrated at a dominant connection point. The passive filters are integrated near the load/dispersed generation components in the scheme; for instance, at a substation. Each one of the passive filters can be considered based on the distorted features related to the load/dispersed generation component. Moreover, according to [21], the active filter is in parallel with the passive filters and the load/dispersed generation sources.

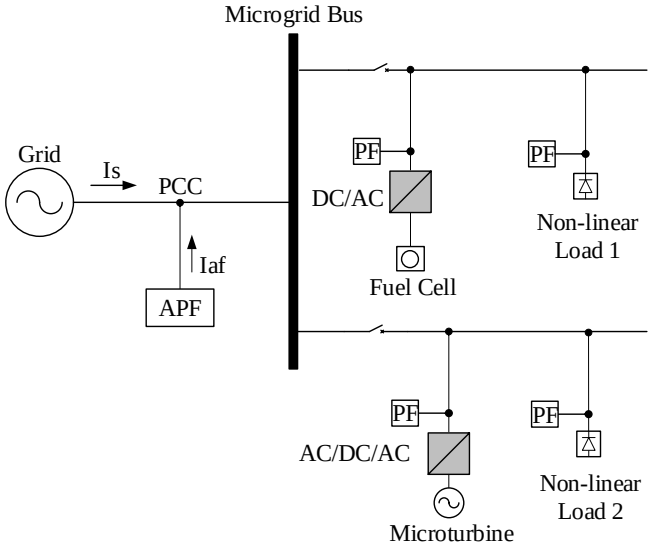

Fig.1. Studied system configuration with nonlinear loads and dispersed generations.

This system contains a sine voltage source along with two DG sources, MT and FC, as well as two non-linear loads, the first of which is formed by three unbalanced single-phase diode rectifiers and the second of which is formed by one three-phase diode rectifier and acts as a source of harmonic current. Further details about the system can be found in Table 1.

TABLE 1. N-Load/DG Parameters and Conditions for the System

Identifier	Components of load/DGs	Current THD%	N-Load Current
Micro turbine	Micro turbine	30.61	Balanced
Fuel cell	Fuel cell	6.08	Balanced
N-Load 1	Three-phase diode rectifier	19.43	Balanced
N-Load 2	Three-phase diode rectifier	19.43	Unbalanced

Fig. 2 shows an MT that has a frequency of 1500 Hz. The MT is just like a normal generator, but its output voltage has a frequency of 1500 Hz. Therefore, the effective voltage of the output phase of this 220 V MT has a frequency of 1500 Hz, but this source cannot be connected to a power system with a frequency of 50 Hz.

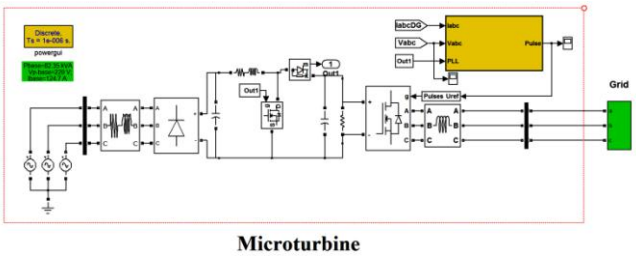

Fig.2. Schematic diagram of the micro turbine.

For this purpose, the input voltage must be rectified using a diode rectifier, and the maximum output voltage of the rectifier will be 530 V. Then, the level of the output voltage can be raised to 750 V using a boost convertor that is connected to an inverter transformer. In Fig. 3, the fuel cell has an output of 50 kW, 625 VDC and is connected to the grid by an AC/DC convertor.

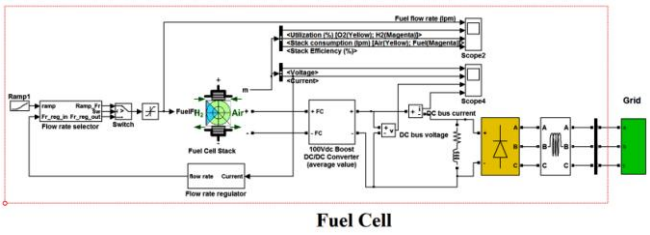

Fig.3. Schematic diagram of the fuel cell

Filter System

A. Passive filter

One-pole and second-order filters are among the most widespread types of passive filters used to remove harmonic currents. The resonant frequency of one-pole filters is close to the harmonic frequency component that must be removed. Second-order filters can remove two harmonic frequencies simultaneously. A second-order damping filter can also be used along with the two filters because it can allow frequency components higher than the filter's cutoff frequency to pass through. Connecting multiple filters in a system can lead to correct impedance specifications of the system. This connection can also affect the filtering of the system, leading to probable resonance in the system [22]. These filters are able to remove the dominant 5th and 7th harmonics. Passive filters have the features of low cost and good efficiency and have been widely used to eliminate the harmonic current of nonlinear loads [21].

B. Active Filter

Using active filters is one the most effective methods for compensating harmonics and reactive power caused by non-linear loads. Active filters are of various types, such as series active filters [23], [24], shunt (parallel) active filters [25], [26] and hybrid active filters (UPQC) [27], [28]. Injecting a harmonic distortion, which is equivalent to a distortion caused by non-linear loads but with an opposite polarity, into the system can lead to correction of the waveform into a sine wave. Voltage distortion results from harmonic current emissions in the system impedance. If a non-linear load with an opposite polarity is injected into the system, the voltage will restore its sinuous form.

Controlling the Active Filters

Several controlling methods have been published in a variety of papers based on frequency and time. Recently, many publications have also appeared on harmonics repression using active power filters. In this paper, the use of three control methods (instantaneous reactive power theory (p-q), DQ synchronous reference frame control (d-q) and Fourier

control method) are applied and compared. Fig. 4 shows an active filter connected to the system in parallel with d-q control method. This active filter can correct the unbalanced current in the system and reduce the input harmonic current. It can also provide the system with the required reactive power in the nominal range, to some extent.

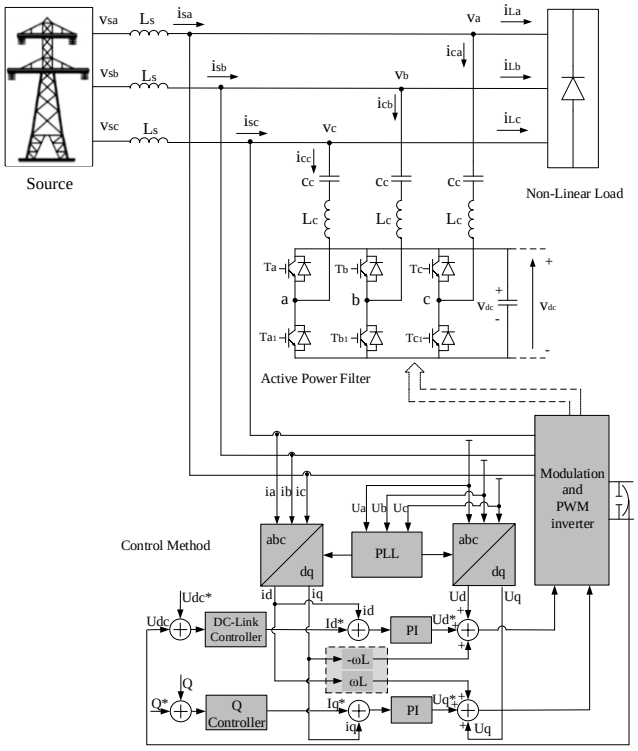

Fig.4. An active power filter with control method for a current harmonic source.

A. Instantaneous Reactive Power Theory

A control method based on instantaneous reactive power theory was first proposed by Akagi in 1984 [29]. This method aimed to fix the instantaneous active power in the feeding network. Instantaneous active and reactive power theories are based on the Clarke transform. The instantaneous three-phase currents and voltages are easily converted into the αβ orthogonal coordinates using the Clarke transform [30], where the α and β axes are the orthogonal coordinates. Vα and Iα are on the α axis, and Vβ and Iβ are on the β axis. The following relations show this conversion:

$$\begin{bmatrix} v_\alpha \\ v_\beta \end{bmatrix} = \sqrt{\frac{2}{3}} \begin{bmatrix} 1 & -1/2 & -1/2 \\ 0 & \sqrt{3}/2 & -\sqrt{3}/2 \end{bmatrix} \begin{bmatrix} v_a \\ v_b \\ v_c \end{bmatrix} \quad (1)$$

$$\begin{bmatrix} i_\alpha \\ i_\beta \end{bmatrix} = \sqrt{\frac{2}{3}} \begin{bmatrix} 1 & -1/2 & -1/2 \\ 0 & \sqrt{3}/2 & -\sqrt{3}/2 \end{bmatrix} \begin{bmatrix} i_a \\ i_b \\ i_c \end{bmatrix} \quad (2)$$

The instantaneous power (p) on the three-phase circuit is defined as follows:

$$p = v_\alpha . i_\alpha + v_\beta . i_\beta \quad (3)$$

where p is equal to the conventional Eq. (4)

$$p = v_a . i_a + v_b . i_b + v_c . i_c \quad (4)$$

The instantaneous reactive power in the $\alpha\beta$ reference frame is defined as:

$$q = v_\alpha \times i_\beta + v_\beta \times i_\alpha \quad (5)$$

where "×" denotes the cross (exterior) product of vectors. Active p and reactive q powers are defined as:

$$\begin{bmatrix} p \\ q \end{bmatrix} = \begin{bmatrix} v_\alpha & v_\beta \\ -v_\beta & v_\alpha \end{bmatrix} \begin{bmatrix} i_\alpha \\ i_\beta \end{bmatrix} \quad (6)$$

Eq. (6) can be rewritten as:

$$\begin{bmatrix} i_\alpha \\ i_\beta \end{bmatrix} = \begin{bmatrix} v_\alpha & v_\beta \\ -v_\beta & v_\alpha \end{bmatrix}^{-1} \begin{bmatrix} p \\ q \end{bmatrix} \quad (7)$$

$v_\alpha . i_\alpha$ and $v_\beta . i_\beta$ in Eq. (6) are instantaneous power, which has been defined by the product of the instantaneous voltage in one axis and the instantaneous current in the same axis [29].

B. Synchronous Reference Frame Control

The Park transformation for electrical power system analysis was extended. The application of the Park transformation to three generic three-phase quantities supplies their components in $dq0$ coordinates [31]. In general, three-phase voltages and currents are transformed into $dq0$ co-ordinates by matrix $[L]$ as follows:

$$\begin{bmatrix} u_d \\ u_q \\ u_0 \end{bmatrix} = [L] \begin{bmatrix} u_A \\ u_B \\ u_C \end{bmatrix} \text{ and } \begin{bmatrix} i_d \\ i_q \\ i_0 \end{bmatrix} = [L] \begin{bmatrix} i_A \\ i_B \\ i_C \end{bmatrix} \quad (8)$$

$$[L] = \sqrt{\frac{2}{3}} \begin{bmatrix} \sin\alpha & \sin\left(\alpha - \frac{2\pi}{3}\right) & \sin\left(\alpha + \frac{2\pi}{3}\right) \\ \cos\alpha & \cos\left(\alpha - \frac{2\pi}{3}\right) & \cos\left(\alpha + \frac{2\pi}{3}\right) \\ \frac{1}{\sqrt{2}} & \frac{1}{\sqrt{2}} & \frac{1}{\sqrt{2}} \end{bmatrix}$$

$$\alpha = \omega t \quad (9)$$

and the three-phase load currents are transformed in $dq0$ co-ordinates by $[L]$

$$\begin{bmatrix} i_{Ld} \\ i_{Lq} \\ i_{L0} \end{bmatrix} = [L] \begin{bmatrix} i_{LA} \\ i_{LB} \\ i_{LC} \end{bmatrix} \quad (10)$$

Therefore, by averaging i_{Ld} and i_{Lq} in domain $[0 - 2\pi]$ results in components i_{Ld} and i_{Lq}, that is

$$\bar{i}_{Ld} = \frac{1}{2\pi}\int_0^{2\pi} i_{Ld}\, d\ \omega t$$
$$\bar{i}_{Lq} = \frac{1}{2\pi}\int_0^{2\pi} i_{Lq}\, d\ \omega t \quad (11)$$

Where

$$i_{Ld} = \sqrt{\frac{2}{3}}\left[\begin{array}{l} i_{LA} sin\ \omega t + i_{LB}\sin\left(\omega t - \frac{2\pi}{3}\right) + \\ i_{LC}\sin\left(\omega t + \frac{2\pi}{3}\right)\end{array}\right] \quad (12)$$

$$i_{Lq} = \sqrt{\frac{2}{3}}\left[\begin{array}{l} i_{LA}\cos\omega t + i_{LB}\cos\left(\omega t - \frac{2\pi}{3}\right) + \\ i_{LC}\cos\left(\omega t + \frac{2\pi}{3}\right)\end{array}\right] \quad (13)$$

$$a_{A1}^{(i)} = \sqrt{\frac{2}{3}}\,\bar{i}_d\,(t)\ and\ \ b_{A1}^{(i)} = \sqrt{\frac{2}{3}}\,\bar{i}_q(t) \quad (14)$$

Equation (14) gives the relationship between the dc component of i_{Ld} and i_{Lq} and the coefficients of i_{LS}, the compensating objective of the APF.

The three-phase load currents are transformed in dq0 co-ordinates as follows

$$\begin{bmatrix} u_d \\ u_q \\ u_0 \end{bmatrix} = [L]\begin{bmatrix} u_A \\ u_B \\ u_C \end{bmatrix} \quad (15)$$

Similarly, the averages of u_d and u_q are calculated, and the coefficients of u_A are

$$a_{A1}^{(u)} = \sqrt{\frac{2}{3}}\,\bar{u}_d\,(t)\ and\ \ b_{A1}^{(u)} = \sqrt{\frac{2}{3}}\,\bar{u}_q(t) \quad (16)$$

Hence, the following equations can be obtained

$$v_d = \frac{2}{3}\left(\begin{array}{l} u_A\sin\omega t + u_B\sin(\omega t - \frac{2\pi}{3}) + \\ u_C\sin(\omega t + \frac{2\pi}{3})\end{array}\right) \quad (17)$$

$$v_d = \frac{2}{3}\left(\begin{array}{l} u_A\cos\omega t + u_B\cos(\omega t - \frac{2\pi}{3}) + \\ u_C\cos(\omega t + \frac{2\pi}{3})\end{array}\right) \quad (18)$$

$$v_0 = \frac{1}{3}(v_A + v_B + v_C) \quad (19)$$

The control variables then become dc values; consequently, filtering and controlling can be easily achieved.

C. Fourier Control Method

By using Fourier analysis as an alternative function of the time domain, discrete frequency components are achieved in the frequency domain. The Fourier integral is defined as:

$$X(f) = \int_{-\infty}^{+\infty} x(t)e^{-j2\pi ft}dt \quad (20)$$

If a Fourier integral is valid for all frequency components, (20) is called a Fourier transform. The Fourier transform is a complex component as:

$$X(f) = RX(f) + jIX(f) \quad (21)$$

where RX (f) and IX (f) are the real and imaginary components, respectively. The magnitude of the x (t) signal's Fourier transform is:

$$|X(f)| = \sqrt{R^2(f) + I^2(f)} \quad (22)$$

The Fourier transform's phase angle (ϕ (f)) is calculated as:

$$\phi(f) = \tan^{-1}\left[\frac{\mathrm{Im}\,X(f)}{\mathrm{Re}\,X(f)}\right] \quad (23)$$

An inverse Fourier transform is defined in (24) as:

$$x(f) = \int_{-\infty}^{+\infty} X(t)e^{j2\pi ft}df \quad (24)$$

Using an inverse Fourier transform, the time domain functions are calculated. The purpose of using a Fourier transform method is to make the source current sinusoidal [32].

Simulation Results

To compare the performance of the three APF control strategies of p-q, d-q, and Fourier under source and load operation conditions, three simulation cases are presented: Case I: the uncompensated system current, case II: the compensated system current after connecting the PF, and case III: the complete compensated system current after connecting the PF and SAPF. The simulation is performed using MATLAB, Simulink, and a sinusoidal grid voltage is assumed.

A. Case I: Unbalanced and Distorted System Currents without any Compensation

For case 1, the resulting system waveforms are shown in Fig. 5 without any compensation. The dispersed generation units (i.e., a micro turbine and a fuel cell) are connected to the system through power electronic converters and nonlinear loads (three-phase and three single-phase diode rectifiers), which produce the distorted waveforms. The DG sources and nonlinear loads make the system current nonlinear and unbalanced.

B. Case II: Unbalanced and Distorted System Currents with a Passive Filter

In case II, each individual PF is connected to a distortion source and is designed to compensate for the major harmonics and to supply reactive power for the distortion source. The simulation results are shown in Fig. 6. The source current is compensated effectively; however, THD value is not in accordance with the standard limits and the unbalanced current has not been compensated. As a result, an active power filter is applied to compensate the remaining harmonics and the unbalanced load.

C. Case III: Balanced and Distorted System Currents with Passive and Active Filters

A system waveform using active and passive filter compensation is shown in Fig. 7. At 0.3 seconds, an active filter is connected to the system, and the system harmonics and unbalanced current are compensated. The p-q, d-q and Fourier control methods are used.

After the active filter is connected, the source current becomes balanced and sinusoidal. The active filter and source current shown in Fig. 7 are obtained using a d-q control method. Because the system voltage is sinusoidal, there is no major difference between the p-q and d-q control method simulation waveforms. As shown (Fourier method), there is no difference between the three control methods with respect to the simulation results. The amount of calculations required, the phase detection circuit and the flexibility at different compensation conditions differ for each control method. For example, phase detection is necessary in d-q control methods, which increases the calculations and complexity, whereas this circuit is not necessary in the p-q methods. Without any compensation system, the current THD is 16.17%; after using compensation, THD is reduced to 3.88% in the p-q method. However, in d-q, it is 6.09% and it is 6.07% in Fourier control methods. Consequently, the p-q control strategy alone is capable of satisfying the IEEE-519 standard harmonic current distortion limits. A detailed summary of the simulation results for the three cases is shown in Table 2.

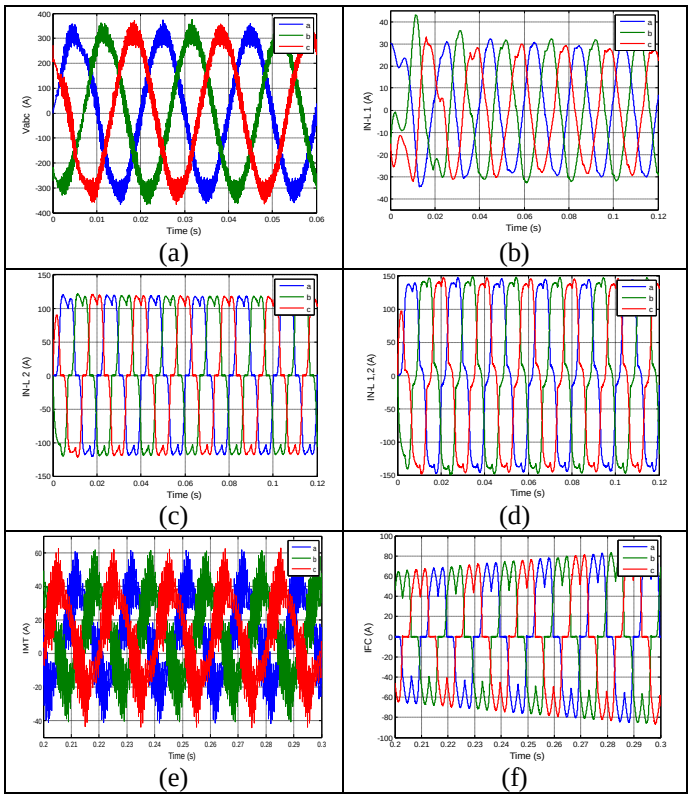

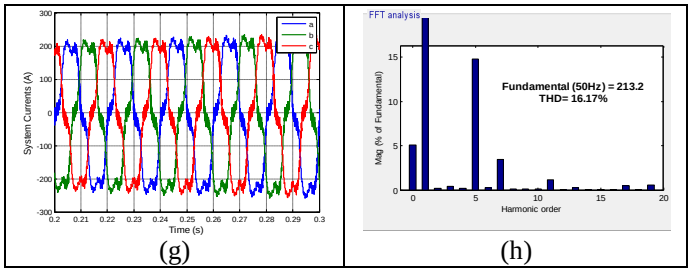

Fig.5. System, DG units and nonlinear loads current waveforms without compensation: (a) voltage source; (b) nonlinear load 1 currents; (c) nonlinear load 2 currents; (d) nonlinear load 1 and 2 currents (together); (e) MT currents; (f) FC currents; (g) system currents; (h) frequency spectrum of the system currents

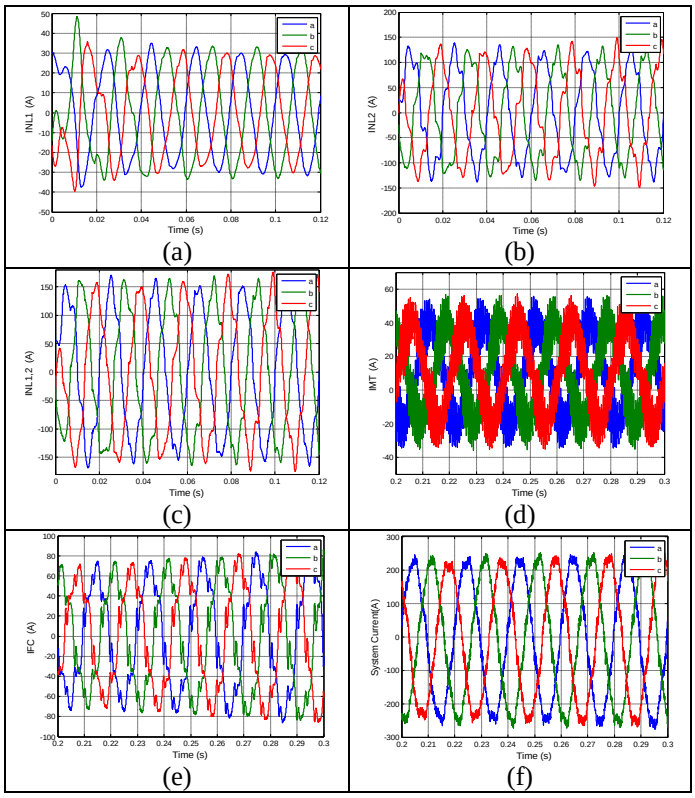

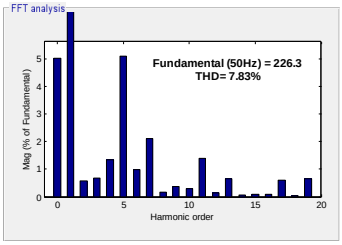

Fig.6. System, DG units and nonlinear loads currents waveforms after passive filter compensation: (a) nonlinear load 1 currents; (b) nonlinear load 2 currents; (c) nonlinear load 1 and 2 currents (together); (d) MT currents; (e) FC currents; (f) system currents; (g) frequency spectrum of the system currents.

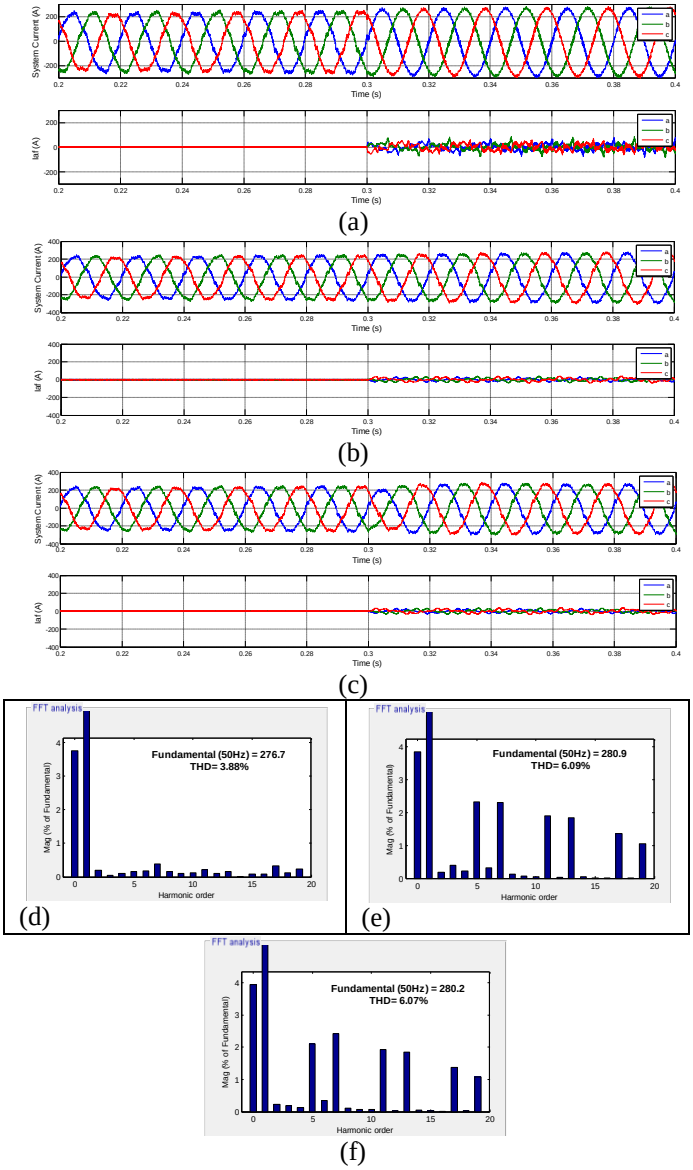

Fig.7. System and active filter currents using (a) p-q, (b) d-q and (c) Fourier control methods and also frequency spectrum of the system currents for them (d), (e) and (f) respectively.

TABLE 2. Simulation Results for the Three Cases

	Current THD (%)					
	N-L1	N-L2	N-L1,2	MT	FC	System
Uncompensated	6.08	19.4	15.4	39.3	30.6	16.17
Passive filter	1.59	9.44	7.73	18.0	17.9	7.83
AF (p-q)	1.41	9.59	7.54	50.1	19.0	3.88
AF (d-q)	1.57	9.04	7.03	39.3	18.4	6.09
AF (Fourier)	1.44	6.97	5.42	40.5	19.1	6.07

Experimental Results

The experimental results aimed to validate the simulation results of the nonlinear control that were obtained for the steady-state operation mode. The experimentation of this work was performed using a test that was designed, developed and implemented in the laboratory. Fig. 8 shows the circuit of single phase hybrid compensator, which includes passive and active filters and a nonlinear load. The current controller that is used in this implementation has a fixed band of DSP-based hysteresis control. The SAPF in this case provides the load reactive power by injecting current. Thus, the source only supplies active power to the load. The real-time performance of the SAPF system with the developed algorithm was tested in the laboratory for several different operating conditions, such as without compensation and with complete compensation. The experimental results are presented in Fig. 9 and are discussed in the following sections.

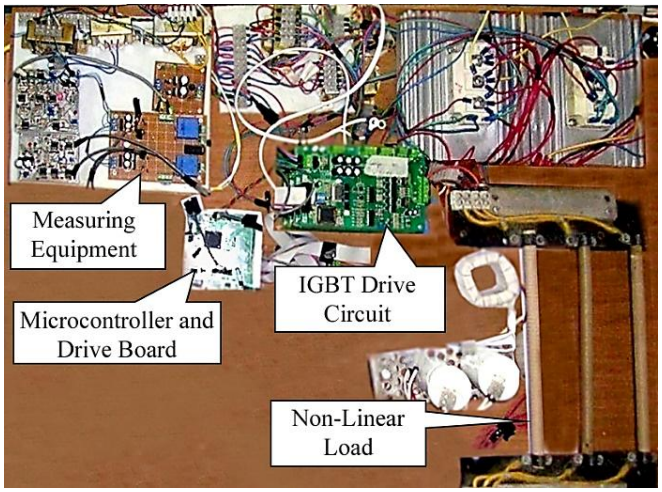

Fig.8. Photography of the APF system prototype

The proposed single phase $d-q$ theory is simulated to confirm the performance with a single-phase SAPF. To validate the simulation results, a scaled 1 kVA single-phase shunt active power filter was operated with the instantaneous reactive power strategy and was implemented using digital signal processor DSP-based hysteresis control ($TMS320F2812\ DSP$). To demonstrate the benefits of $TMS320F2812$, the configurations are compared with the ordinary model of ATMEGA32 DSP. For example, in $TMS320F2812$, the frequency (MHz), flash (KB), PWM (Ch) and pin/package are 150, 256, 16 and 176, but in the ordinary model, their values are 16, 32, 2 and 40, respectively. The DSP calculates the reference voltage for the APF and then generates PWM gate signals for the six IGBT ($s_1, s_2, s_3, s_1^{'}, s_2^{'}, s_3^{'}$) switches. The sampling time used in the practical test for the proposed system is 40 µs. The average switching frequency (f_s) at which the inverter was working was between 5 and 7 kHz.

Fig. 9 shows the experimental results waveform: (a) a distorted voltage source (v_{pcc}) and nonlinear load current (i_L), (b) a load current and compensation source current (i_s) and (c) an active power filter current (i_c) and compensation source current. In case (a), (v_{pcc}) is considered as distorted with a voltage THD of 12.5%, and i_L has a THD of 28.4%. Fig. 9 (b) (c) shows the nonlinear load current i_L, source current i_s and SAPF current i_c waveforms after SAPF compensation. Fig. 9 b shows the experimental results with a nonlinear load

connected to the system. The load current has a THD of 28.4% with dominant 5th and 7th harmonics. The source current profile shows the significant presence of harmonics, even after the SAPF is in operation. In Fig. 9 (c), with complete compensation, the SAPF effectively removes the harmonics due to the nonlinear load by injecting an appropriate current such that the nonlinear load appears almost as a linear resistive load. The source current has a THD of 3.8%. There is significant improvement in the waveform of the source current in comparison with the load current waveform. After compensation, i_s becomes sinusoidal and in-phase with the v_{pcc}, which shows effective compensation of the harmonic distortion and reactive power. The THD level of i_s is reduced from 28.4% (before any compensation) to 3.8% (with complete compensation).

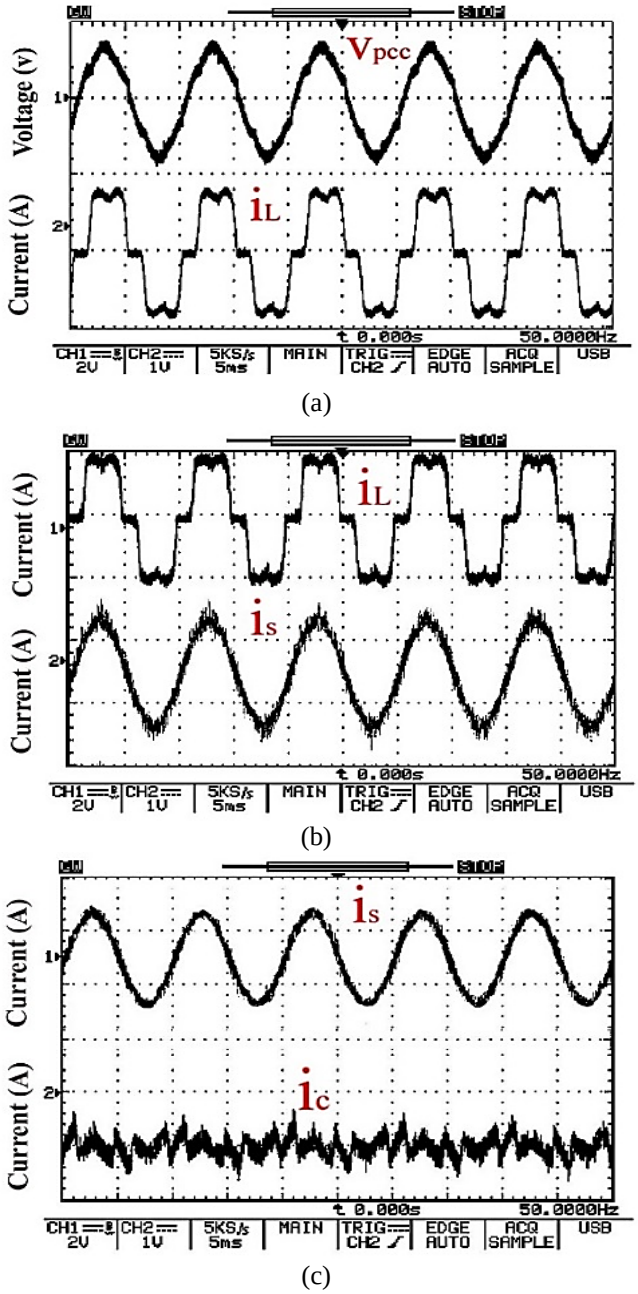

Fig.9. Single-phase shunt active power filter waveforms under distorted PCC voltage.

Fig. 9 (a – c) present the experimental results showing that nearly identical waveforms to the simulation waveforms are obtained when using the same parameters. The parameters used in the system are given in Table 3.

TABLE 3. Experimental parameters of the System

Parameter	Values
AC supply voltage (V)	35
AC inductor of the diode rectifier: (Lac) (mH)	5
AC resistor of the diode rectifier: (Rac) (Ω)	3
System resistance: Rs (Ω)	0.3
Load resistance: RL (Ω)	165
Active filter ripple filter inductance Rf (Ω)	12
Line frequency (Hz)	50
System equivalent inductance: Ls (mH)	0.30
Load input inductor: Lac (mH)	3.8
DC capacitor: Cdc (µf)	470
Average switching frequency: fs (kHz)	6

Once the APF is connected to the PCC, the current becomes sinusoidal, and the reactive power also becomes compensated. These figures indicate that the experiment results are similar to the simulation results, which proves the better performance of the proposed active power filter system with the control strategy.

Conclusion

A group of nonlinear loads as harmonic current sources are discussed in this paper. These loads produce disturbances of the power system voltage and current. As a result, passive and active filters are proposed to eliminate the harmonic issues. Passive filters are employed to remove the dominant third and fifth harmonic components and to compensate the load reactive power, whereas active filters are applied to compensate the remaining harmonic components and negative sequence. The simulation results demonstrated that the system current THD was reduced below 5% by the p-q method, which meets the IEEE-519 and CEI 61000 standard limits. An experimental investigation based on a prototype single-phase active power filter has been conducted to confirm the performance of the APF with an instantaneous reactive power strategy.

Acknowledgments

The authors would like to thank Universiti Teknologi Malaysia for the support and management under vote 10H58. Moreover, wewould also like to thank the Malaysian Ministry of Education (MOE) for the cooperation and financial support for doing this work.

References

[1] H. Akagi, “Active harmonic filters,” *Proc. IEEE*, vol. 93, no. 12, pp. 2128–2141, 2005.

[2] A. Naderipour and A. Asuhaimi Mohd Zin, "The Peruse of Designing a Hybrid Filter to Omission Harmonics and Reactive Power Improvement in Distributed Generation systems," in *2nd International Conference on Power Engineering, Control and Mechatronics (MIC-PCM 2012)*, 2012, vol. 2, no. 1, pp. 6–7.

[3] F. Z. Peng, "Harmonic sources and filtering approaches," *Ind. Appl. Mag. IEEE*, vol. 7, no. 4, pp. 18–25, 2001.

[4] C.-L. Su and C.-J. Hong, "Design of passive harmonic filters to enhance power quality and energy efficiency in ship power systems," in *Industrial & Commercial Power Systems Technical Conf (I&CPS), 2013 IEEE/IAS 49th*, 2013, pp. 1–8.

[5] H. M. Zubi, R. W. Dunn, and F. V. P. Robinson, "Comparison of different common passive filter topologies for harmonic mitigation," in *Universities Power Engineering Conference (UPEC), 2010 45th International*, 2010, pp. 1–6.

[6] J. F. Cline and B. M. Schiffman, "Tunable passive multicouplers employing minimum-loss filters," *Microw. Theory Tech. IRE Trans.*, vol. 7, no. 1, pp. 121–127, 1959.

[7] S. Biricik and Ö. C. Özerdem, "Harmonic distortion comparison of switched capacitors with active power filter for reactive power compensation," in *Environment and Electrical Engineering (EEEIC), 2010 9th International Conference on*, 2010, pp. 269–272.

[8] J. G. Linvill, "RC active filters," *Proc. IRE*, vol. 42, no. 3, pp. 555–564, 1954.

[9] N. Santos, W. Ricardo, E. R. Cabral da Silva, C. Brandao Jacobina, E. de Moura Fernandes, A. Cunha Oliveira, R. Rocha Matias, F. Guedes Filho, O. M. Almeida, and P. Marinho Santos, "The transformerless single-phase universal active power filter for harmonic and reactive power compensation," *Power Electron. IEEE Trans.*, vol. 29, no. 7, pp. 3563–3572, 2014.

[10] M. Waware and P. Agarwal, "Hardware Realization of Multilevel Inverter-based Active Power Filter," *IETE J. Res.*, vol. 58, no. 5, pp. 356–366, 2012.

[11] N. Balbo, D. Sella, R. Penzo, G. Bisiach, D. Cappellieri, L. Malesani, and A. Zuccato, "Hybrid active filter for parallel harmonic compensation," in *Power Electronics and Applications, 1993., Fifth European Conference on*, 1993, pp. 133–138.

[12] M. Salehifar, H. A. Mohammadpour, A. H. Moghadasi, and A. Shoulaie, "Harmonic elimination in single phase systems by means of a hybrid series active filter (HSAF)," in *Power Electronic & Drive Systems & Technologies Conference (PEDSTC), 2010 1st*, 2010, pp. 423–428.

[13] S. K. Tso and M. H. Rashid, "Simulation of a fast-acting reactive current compensator," *Electr. Mach. Power Syst.*, vol. 13, no. 6, pp. 409–419, 1987.

[14] A. Naderipour and A. Jalilian, "Designing a Hybrid Compensator to Eliminate Harmonics and Control Reactive Power in Distributed Generation Systems," *Int. Rev. Model. Simulations*, vol. 4, no. 2, 2011.

[15] A. R. Naderipour, "A hybrid solution to improve power quality in dispersed generation systems," in *Power Quality Conference (PQC), 2010 First*, 2010, pp. 1–4.

[16] T. C. Green and J. H. Marks, "Control techniques for active power filters," *IEE Proceedings-Electric Power Appl.*, vol. 152, no. 2, pp. 369–381, 2005.

[17] Y.-M. Chen, H.-C. Wu, Y.-C. Chen, K.-Y. Lee, and S.-S. Shyu, "The AC line current regulation strategy for the grid-connected PV system," *Power Electron. IEEE Trans.*, vol. 25, no. 1, pp. 209–218, 2010.

[18] N. Jelani and M. Molinas, "Shunt active filtering by constant power load in microgrid based on IRP pq and CPC reference signal generation schemes," in *Power System Technology (POWERCON), 2012 IEEE International Conference on*, 2012, pp. 1–6.

[19] D. J. Hogan, F. Gonzalez-Espin, J. G. Hayes, G. Lightbody, and M. G. Egan, "Adaptive resonant current-control for active power filtering within a microgrid," in *Energy Conversion Congress and Exposition (ECCE), 2014 IEEE*, 2014, pp. 3468–3475.

[20] D. Menniti, A. Burgio, A. Pinnarelli, and N. Sorrentino, "Grid-interfacing active power filters to improve the power quality in a microgrid," in *Harmonics and Quality of Power, 2008. ICHQP 2008. 13th International Conference on*, 2008, pp. 1–6.

[21] Z. Chen, F. Blaabjerg, and J. K. Pedersen, "Hybrid compensation arrangement in dispersed generation systems," *Power Deliv. IEEE Trans.*, vol. 20, no. 2, pp. 1719–1727, 2005.

[22] J. C. Das, "Passive filters-potentialities and limitations," in *Pulp and Paper Industry Technical Conference, 2003. Conference Record of the 2003 Annual*, 2003, pp. 187–197.

[23] M. A. Mulla, C. Rajagopalan, and A. Chowdhury, "Compensation of three-phase diode rectifier with capacitive filter working under unbalanced supply conditions using series hybrid active power filter," *Power Electron. IET*, vol. 7, no. 6, pp. 1566–1577, 2014.

[24] L. Guohai, D. Yun, Q. Peng, C. Zhaoling, C. Shanghao, and S. Yue, "NPC three-level series active power filter with neutral-point voltage self-restraining," in *Control Conference (CCC), 2014 33rd Chinese*, 2014, pp. 6978–6981.

[25] Q.-N. Trinh and H.-H. Lee, "Versatile Shunt Hybrid Power Filter to Simultaneously Compensate Harmonic Currents and Reactive Power," *J. Electr. Eng. Technol.*, vol. 10, no. 3, pp. 1311–1318, 2015.

[26] G. W. Chang, R. C. Hong, and H. J. Su, "IEEE standard 1459-based reference compensation current strategy for three-phase three-wire shunt active power filter control," in *Harmonics and Quality of Power (ICHQP), 2014 IEEE 16th International Conference on*, 2014, pp. 551–555.

[27] S. Khadem, M. Basu, and M. Conlon, "Intelligent Islanding and Seamless Reconnection Technique for Microgrid with UPQC."

[28] S. Kaliappan, M. Poornima, and R. Rajeswari, "Improvement of source voltage and load current harmonic mitigation using UPQC: A survey," in *Intelligent Systems and Control (ISCO), 2013 7th International Conference on*, 2013, pp. 110–114.

[29] H. Akagi, Y. Kanazawa, and A. Nabae, "Instantaneous reactive power compensators comprising switching devices without energy storage components," *Ind. Appl. IEEE Trans.*, no. 3, pp. 625–630, 1984.

[30] M. Aredes and E. H. Watanabe, "New control algorithms for series and shunt three-phase four-wire active power filters," *Power Deliv. IEEE Trans.*, vol. 10, no. 3, pp. 1649–1656, 1995.

[31] R. S. Herrera, P. Salmerón, and H. Kim, "Instantaneous reactive power theory applied to active power filter compensation: Different approaches, assessment, and experimental results," *Ind. Electron. IEEE Trans.*, vol. 55, no. 1, pp. 184–196, 2008.

[32] J. D. Bruce, "Discrete Fourier transforms, linear filters, and spectrum weighting," *Audio Electroacoust. IEEE Trans.*, vol. 16, no. 4, pp. 495–499, 1968.